RESILIENCY OF AN AIR-FLOATED WEB

by

Y. B. Chang[1], R. P. Swanson[2] and P. M. Moretti[1]
[1]Oklahoma State University
[2]3M Company
USA

ABSTRACT

Air-flotation ovens are used for non-contact drying of coated web materials such as photographic film, magnetic media, and paper. In a typical air-flotation oven, the air bars are arranged in such a way that the path of web is nearly sinusoidal. When web tension fluctuates, the distance between the web and the air bars also changes. This phenomenon affects the longitudinal dynamics and tension control of an air-floated web. In some cases, tension fluctuations can cause the web to touch the air bars, resulting in damage to the coating and the web. This paper discusses an analytical model of the extensional resiliency of an air-floated web. The analysis shows that at low tension the machine-directional stiffness of an air-floated web is small, being dominated by the air cushion effects. At higher web tensión, however, the effects of material deformation become more important than the air cushion effects. The analysis is compared with the experimental results obtained in a pilot air-flotation oven. The analytical and experimental results show the same trends, though the analytical model tends to underpredict the longitudinal stiffness of air-supported web.

NOMENCLATURE

d	Web width
E	Modulus of elasticity; $\sigma_x(1-v^2)/\varepsilon_x$ for plane stress
E_o	Apparent modulus of elasticity defined as σ_x/ε_x
e	Vertical distance (gap) between the upper and lower rows of air bars
F_x	Longitudinal force on the web; $F_x = T \cdot d$
h	Effective flotation height; vertical distance between web and the exit of air jet

h_l	Minimum vertical distance between web and air bar, i.e., clearance of web
h_o	Maximum vertical distance between web and air bar
p_j	Total pressure of air jet at the nozzle; $p_j = Cp_o$
p_o	Supply pressure of air inside air bar
F	Out-of-plane aerodynamic force generated by an air bar
L_{oven}	Length of oven
L_{web}	Total length of web
$L_{web,in}$	Length of web inside the oven
$L_{web,out}$	Length of web outside the oven
N	Number of air bars in oven
s	Vertical distance between the top surface of air bar and the exit of air jet
T	Web tension (longitudinal force per unit width of web)
x	Longitudinal axis
w	Width of air bar (distance between two slot nozzles)
z	Out-of-plane deflection profile of web
α	Longitudinal angle of web at the center of two adjacent air bars
δ	Total longitudinal deflection of web
ε_x	Longitudinal strain in the web
λ	Pitch of air bars (distance between two adjacent air bars in the same row); $\lambda = 2L_{oven} / N$
ν	Poisson's ratio
θ	Angle of ejection of air jet
σ_x	Longitudinal stress in the web

INTRODUCTION

Air-flotation ovens are used for noncontact drying of coated web materials such as photographic films, magnetic media, and paper. The key components in air-flotation ovens are air bars which emit hot gases for noncontact supporting and drying the coated materials. In typical air-flotation ovens, the air bars are arranged in such a way that the paths of web are nearly sinusoidal as indicated in Figure 1. The amplitude of the sinusoidal curve depends on the design of air bars, the arrangement of air bars, supply pressure of air, and web tension. When web tension increases, the distance between the web and air bars is reduced and so is the amplitude of the sinusoidal curve. Therefore, when tension fluctuates, air-floated webs experience much greater strains than roller-supported web spans. This phenomenon affects the longitudinal dynamics of an air-floated web and its control. Tension fluctuation can also cause other problems such as touchdowns and touchups in an oven. In order to avoid contacts between the web and air bars, the out-of-plane stiffness of the air-floated web must be large.

An analytical model is developed in this paper for prediction of both the out-of-plane and longitudinal resiliencies of an air-floated web. This prediction model is based on the study of aerodynamic characteristics explained in Chang and Moretti [1]. The model is

compared with experimental results obtained from a pilot air-flotation oven.

ANALYSIS

Geometric Relationships

When the out-of-plane deflection of the web is much smaller than the pitch of air bars, the web deflection profile can be approximated as

$$z = \left(h_o - \frac{e}{2}\right)\sin\frac{2\pi x}{\lambda} \qquad \{1\}$$

As defined in Figure 1 and Figure 2, h_o is the maximum gap between the web and the air bars, e is the vertical distance between the upper and lower rows of air bars, and λ is the distance between two adjacent air bars in the same row. The slope of the web at the center of two adjacent air bars is

$$\tan\alpha = \left[\frac{dz}{dx}\right]_{x=0} = \frac{2\pi\left(h_o - e/2\right)}{\lambda} \qquad \{2\}$$

Out-of-Plane Force Balance

If we assume that the web is not deformed in the lateral direction and the web tension T is uniform, the equation for the out-of-plane force balance is

$$2T\sin\alpha = F \qquad \{3\}$$

where F is the lift force per unit width of web for one air bar.

Aerodynamic Lift Force

The aerodynamic lift force per unit width of air-floated web, as explained in Chang and Moretti [1], is

$$F = p_j b\left[1 - \exp\left\{\left(-\frac{2b}{h}\right)(1+\cos\theta)\right\}\right]\left(\frac{w}{b} + \frac{h}{b}\frac{2\sin\theta}{1+\cos\theta}\right) \qquad \{4\}$$

where h is the effective flotation height defined as the vertical distance between the exit of air jet and the web as shown in Figure 2, and θ is the ejection angle of air jets. The effective flotation height h can be written as

$$h = \left(h_o - \frac{e}{2}\right)\sin\left(\frac{\pi}{2} - \frac{\pi w}{\lambda}\right) + \frac{e}{2} + s \qquad \{5\}$$

from which

$$\frac{dh}{dh_o} = \sin\left(\frac{\pi}{2} - \frac{\pi w}{\lambda}\right)$$ {6}

Touchdowns and touchups in an air-flotation oven are related to the minimum distance between the web and air bars. The minimum vertical distance between the web and air bars (or clearance of web) can be written as

$$h_1 = \left(h_o - \frac{e}{2}\right)\sin\left(\frac{\pi}{2} - \frac{\pi w}{\lambda}\right) + \frac{e}{2}$$ {7}

Flotation Height and Web Tension: Out-of-Plane Resiliency

The flotation height can be determined from the out-of-plane force balance condition (Eq. {3}), the total lift force generated by an air bar (Eq. {4}), and the geometrical relationship (Eq. {2}) as follows:

$$T = \left(\frac{p_j b \lambda}{4\pi}\right)\frac{1}{(h_o - e/2)}\left[1 - \exp\left\{\left(-\frac{2b}{h}\right)(1 + \cos\theta)\right\}\right]\left(\frac{w}{b} + \frac{h}{b}\frac{2\sin\theta}{1 + \cos\theta}\right)$$ {8}

The out-of-plane stiffness associated with the minimum flotation height is

$$\frac{dT}{dh_1} = \frac{dT}{dh_o}\frac{dh_o}{dh_1} = \frac{dT}{dh_o}\frac{1}{\sin\left(\frac{\pi}{2} - \frac{\pi w}{\lambda}\right)}$$ {9}

where dT/dh_o is obtained from Eq. {8} as

$$\frac{dT}{dh_o} = -\left(\frac{p_j b \lambda}{4\pi}\right)\frac{1}{(h_o - e/2)^2}\left[1 - \exp\left\{\left(-\frac{2b}{h}\right)(1 + \cos\theta)\right\}\right]\left(\frac{w}{b} + \frac{h}{b}\frac{2\sin\theta}{1 + \cos\theta}\right)$$

$$-\left(\frac{p_j b \lambda}{4\pi}\right)\frac{1}{(h_o - e/2)}\frac{2b}{h^2}\exp\left\{\left(-\frac{2b}{h}\right)(1 + \cos\theta)\right\}\frac{dh}{dh_o}\left(\frac{w}{b} + \frac{h}{b}\frac{2\sin\theta}{1 + \cos\theta}\right)$$ {10}

$$+\left(\frac{p_j b \lambda}{4\pi}\right)\frac{1}{(h_o - e/2)}\left[1 - \exp\left\{\left(-\frac{2b}{h}\right)(1 + \cos\theta)\right\}\right]\frac{2\sin\theta}{b(1 + \cos\theta)}$$

Resiliency of web is the inverse of stiffness, that is, dh_1/dT.

Longitudinal Deflection and Web Tension: Longitudinal Resiliency

If we assume $z_{max} \ll \lambda$, the actual length of web contained in one pitch of air bars can be written as

$$L_\lambda = \int_0^\lambda \sqrt{1 + \left(\frac{dz}{dx}\right)^2}\, dx$$

$$\approx \int_0^\lambda \left[1 + 2\pi^2 \left(\frac{h_o - e/2}{\lambda}\right)^2 \cos^2 \frac{2\pi x}{\lambda}\right] dx \qquad \{11\}$$

$$= \lambda\left[1 + \pi^2 \left(\frac{h_o - e/2}{\lambda}\right)^2\right]$$

so that the total length of web in an oven is

$$L_{web,in} = \frac{L_{oven}}{\lambda} L_\lambda = L_{oven}\left[1 + \pi^2 \left(\frac{h_o - e/2}{\lambda}\right)^2\right] \qquad \{12\}$$

and

$$\frac{dL_{web,in}}{dh_o} = L_{oven}\pi^2 \frac{d}{dh_o}\left[\left(\frac{h_o - e/2}{\lambda}\right)^2\right] = 2\pi^2 \left(\frac{h_o - e/2}{\lambda}\right)\left(\frac{L_{oven}}{\lambda}\right) \qquad \{13\}$$

The aerodynamic equivalent spring constant per unit width of web is

$$k_{air} = -\frac{dT}{dL_{web,in}} = -\frac{dT}{dh_o}\frac{dh_o}{dL_{web,in}} = -\frac{dT}{dh_o}\left(\frac{1}{2\pi^2}\right)\left(\frac{\lambda}{h_o - e/2}\right)\left(\frac{\lambda}{L_{oven}}\right) \qquad \{14\}$$

If E, v, and t are the modulus of elasticity, Poisson's ratio, and the thickness of the web, respectively, then the spring constant per unit width of web related to the elastic deformation is

$$k_{elas} = \frac{dT}{dL_{web}} = \frac{tE_o}{\left(L_{web,in} + L_{web,out}\right)} = \frac{tE_o}{\left\{L_{oven}\left[1 + \pi^2 \left(\frac{h_o - e/2}{\lambda}\right)^2\right] + L_{web,out}\right\}} \qquad \{15\}$$

The total spring constant per unit width of web becomes

$$k_{eff} \equiv \frac{dT}{d\delta} = \frac{k_{air}k_{elas}}{k_{air} + k_{elas}} \qquad \{16\}$$

EXAMPLE CALCULATIONS

Design and Operating Conditions

An application of the analytical model discussed in this paper is demonstrated by considering a typical example of air-flotation ovens. The type of air bars considered in these example calculations is the same as one of the commercial models discussed in Chang and Moretti [1]. The main design and operating parameters can be divided into four groups and their values considered in the calculations are as follows:

Characteristics of individual air bars

$w = 0.127$ m

$b = 0.0033$ m

$s = 0.0033$ m

$\theta = 90°$

$C = 0.85$

Characteristics of oven

$L_{oven} = 10.16$ m

$N = 40$

$\lambda = 2L_{oven} / N = 0.508$ m

-5 mm $\leq e \leq 10$ mm

Web properties and dimensions

$E_o = \dfrac{\sigma_x}{\varepsilon_x} = 4.41 \cdot 10^9 \, Pa$

$d = 1.524$ m

$t = 37.1 \, \mu m$

$L_{web,out} = 0.762$ m

Operating conditions

$p_o = 620, 1240, 1870$ and 2490 Pa

$T = $ Variable

Calculation Results

The minimum vertical distance between the web and the air bars is plotted in Figure 3 as a function of web tension for various values of supply air pressure for $e = 0$ mm. When the web tension is small or when the flotation height is big, a small increase of tension results in a big reduction of flotation height. The effect of tension variation

becomes smaller at high web tension. On the other hand, Figure 4 shows that the clearance of web is almost linearly proportional to the supply pressure. The gap between the upper and lower rows of air bars also appears to strongly affect the clearance as shown in Figure 5. When e is negative (surface of the upper air bars is below the level of the surface of lower air bars), the clearance reduces quickly as tension increases. For example, when e = -5 mm, the web should touch air bars when then tension is larger than T = 2630 N/m (this value is beyond the range of T in Figure 5). Note that the clearance should approach e/2 if e is positive and web tension is very large. Therefore, unless there is a tremendous benefit in heat transfer, the gap between the upper and lower rows of air bars should not be made negative. The curves for the out-of-plane stiffness are shown in Figure 6. It is seen that the stiffness increases when the supply air pressure is reduced. This trend is due to the fact that when the supply pressure is low, the flotation height is quickly reduced with the increase in web tension, and the longitudinal stretching is little more than the actual strain in the web material.

The longitudinal stiffness, $dT/d\delta$, is shown in Figure 7 as a function of web tension for various values of supply air pressure. Note that the longitudinal stiffness, just like the out-of-plane stiffness, increases when the supply pressure is reduced. On the other hand, the effects of the gap between the upper and lower air bars are almost negligible as seen in Figure 8.

EXPERIMENTAL VERIFICATION

Test Setup and Procedure

The first step was to evaluate the elastic property of the web material. As shown in Figure 9, the elongation of the web was measured for various values of tensile force. Note that it is difficult to exactly define the elongation of the web because a slack web deforms so much when a tensile force starts to be applied. Ignoring those data points for small tensile force, the slope of the best-fit linear curve is obtained as $dF_x/d\delta = 4400$ N/m. If we assume a plane stress condition and assume $v = 0.4$, the modulus of elasticity is

$$E = \frac{\sigma_x}{\varepsilon_x}\left(1 - v^2\right) = \frac{dF}{d\delta}\frac{L}{td}\left(1 - v^2\right) = 3.72 \cdot 10^9 \, \text{Pa} \qquad \{17\}$$

It is not necessary to evaluate the exact value of modulus of elasticity because, for comparison of the theory and experimental data, we can use the apparent modulus of elasticity defined as

$$E_o = \frac{\sigma_x}{\varepsilon_x} = 4.41 \cdot 10^9 \, \text{Pa} \qquad \{18\}$$

A portion of the air-flotation oven was used for the main experiments. The active region was 4.95 m long and contained 16 pressure-pad air bars. Test conditions are as follows:

549

Characteristics of individual air bars

w = 0.127 m

b = 0.0033 m

s = 0.0033 m

$\theta = 90°$

C = 0.85

Characteristics of oven

L_{oven} = 4.95 m

N = 16

$\lambda = 2L_{oven} / 16 = 0.620$ m

e = 0, 6.4 mm

Web properties and dimensions

$$E_o = \frac{\sigma_x}{\varepsilon_x} = 4.41 \cdot 10^9 \, Pa$$

d = 0.254 m

t = 37.1 μm

$L_{web,out}$ = 4.51 m

Operating conditions

p_o = 620, 1240, and 1870 Pa

T = Variable

Measurement Results

We repeated the measurement of the elongation of the air-floated web for various values of web tension, gap between the upper and lower rows of air bars, and supply air pressure. The air was at room temperature. The longitudinal stiffness was determined as $k_{eff,exp} = \Delta T / \Delta \delta$. Figure 10 through Figure 12 show the measured data and the prediction curve for three different values of supply air pressure. In all cases, the gap between the upper and lower rows of air bars was zero (e = 0 mm). It is seen that the analytical and experimental results show the same trend, though the predicted values of longitudinal stiffness appear to be a little lower than measurements. When the gap between the upper and lower rows of air bars is e = 6.4 mm, as shown in Figure 13 to Figure 15, the prediction seems to follow the same trend of the measurement data, but the prediction curves fall below the measured stiffness values with slightly bigger discrepancies compared to the cases for e = 0 mm.

550

CONCLUSIONS

An analytical model has been developed for prediction of both the out-of-plane and longitudinal stiffness (inverse of resiliency) of a web in air-flotation ovens. The longitudinal stiffness was measured in a pilot air-flotation oven for various values of web tension, gap between the upper and lower rows of air bars, and supply air pressure. It is found that the analytical and experimental results show the same trend, but the theory tends to underpredict the longitudinal stiffness of a web in air-flotation ovens.

REFERENCE

1. Chang, Y. B. and Moretti, P. M., "Aerodynamic Characteristics of Pressure-Pad Air Bars." ASME AD-Vol. 53-2, Fluid-Structure Interactions, Aeroelasticity, Flow-Induced Vibration & Noise, Vol. II, pp. 3-9. Presented at the Fourth International Symposium on Fluid-Structure Interactions, Aeroelasticity, Flow-Induced Vibration & Noise, Dallas, Texas, November 17-21, 1997.
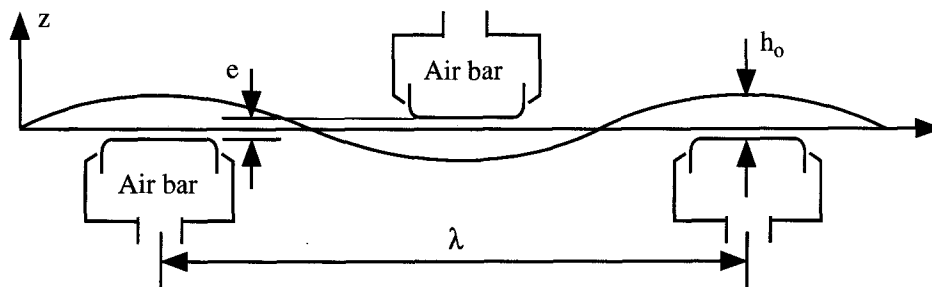
Figure 1. Schematic of air bars and air-floated web
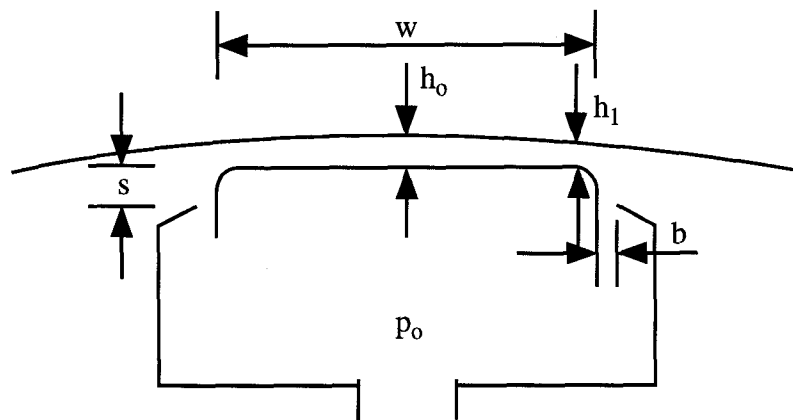
$$w = 127 \text{ mm}, \ b = s = 3.3 \text{ mm}$$

Figure 2. Cross sectional view of a typical air bar
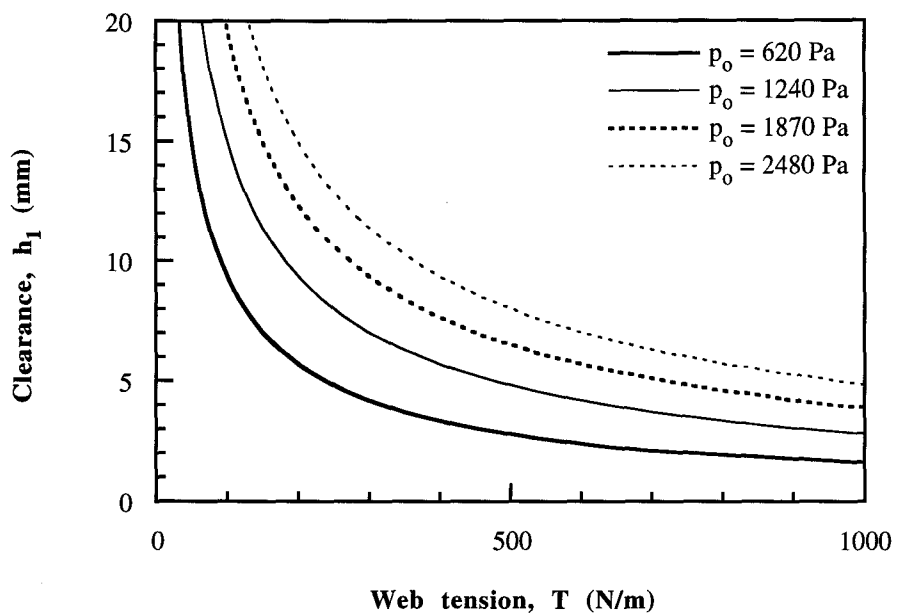
Figure 3. Effects of web tension and supply air pressure on clearance (e = 0 mm)
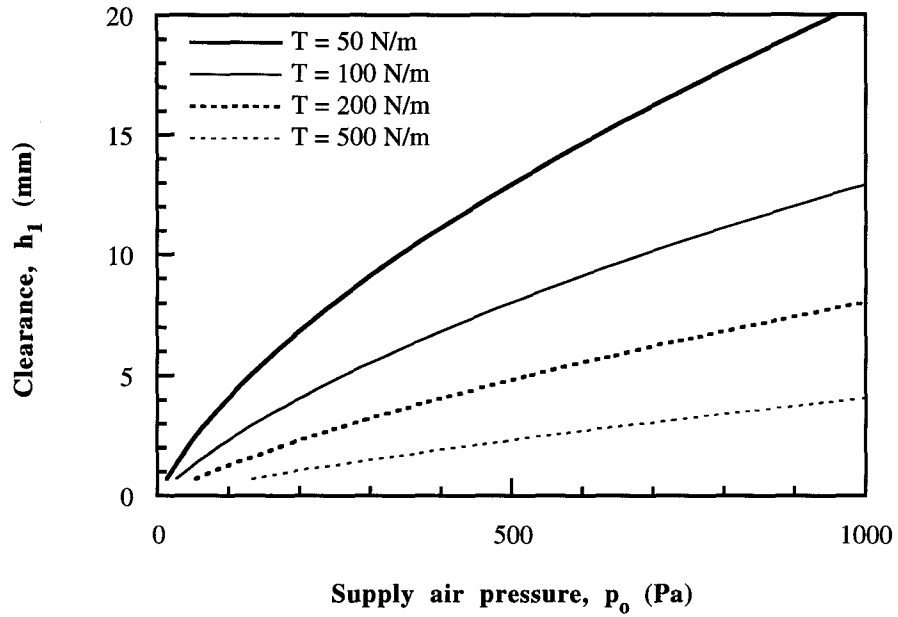
Figure 4. Effects of web tension and supply air pressure on clearance (e = 0 mm)
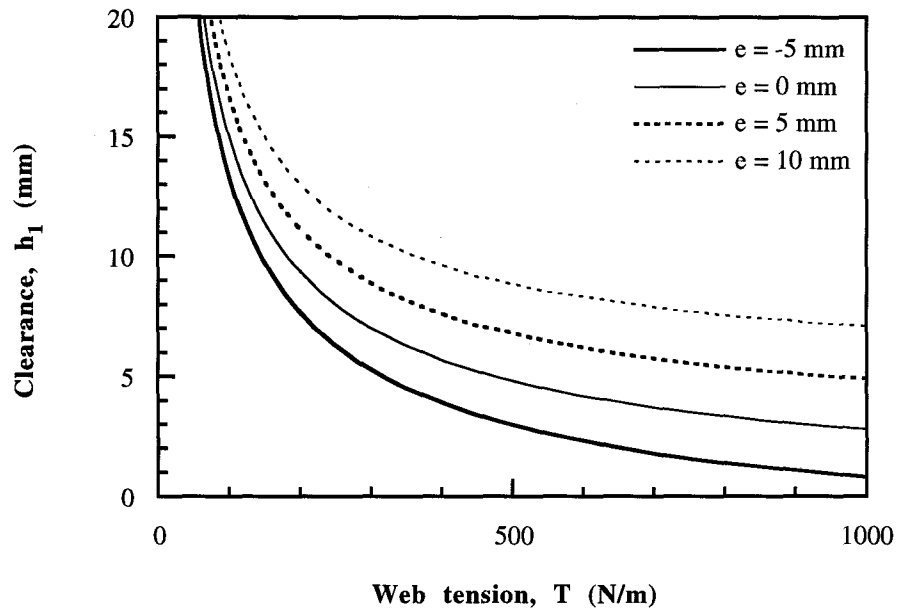
Figure 5. Effects of web tension and the gap between the upper and lower rows of air bars
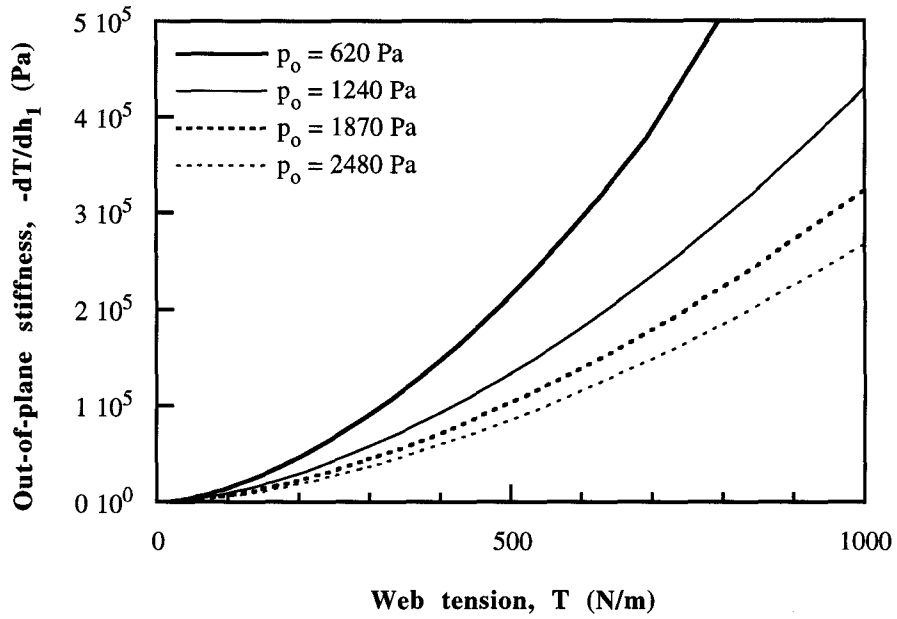on clearance (p_o = 1240 Pa)

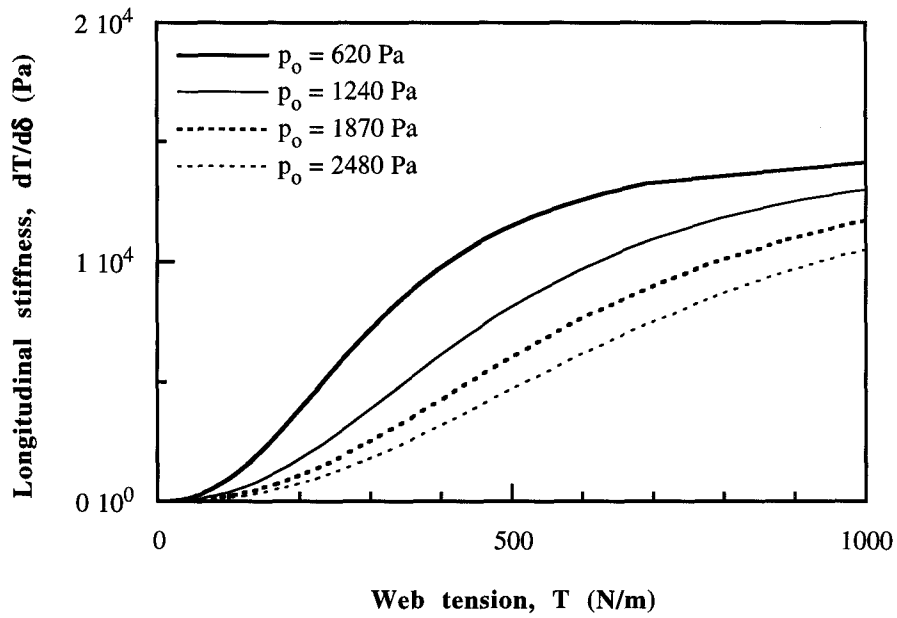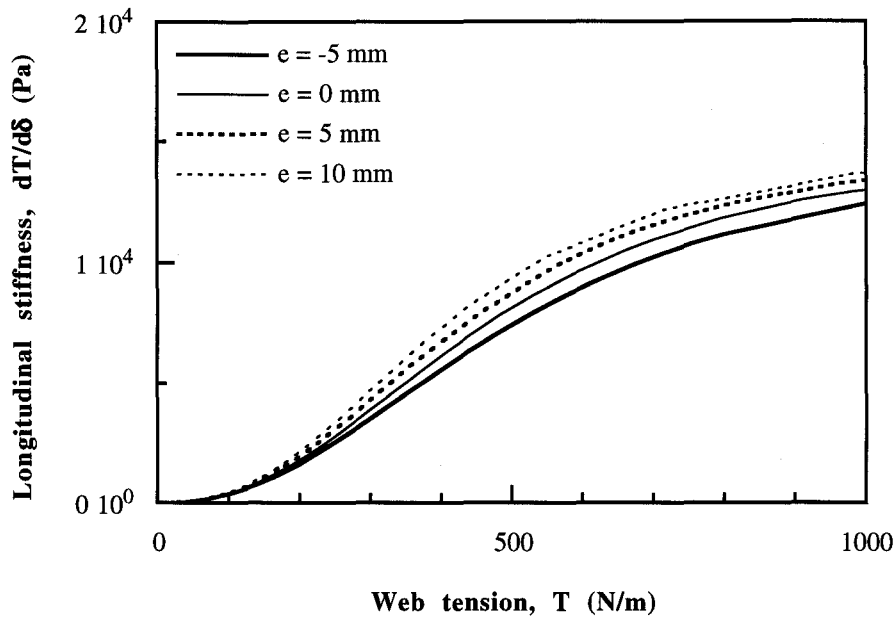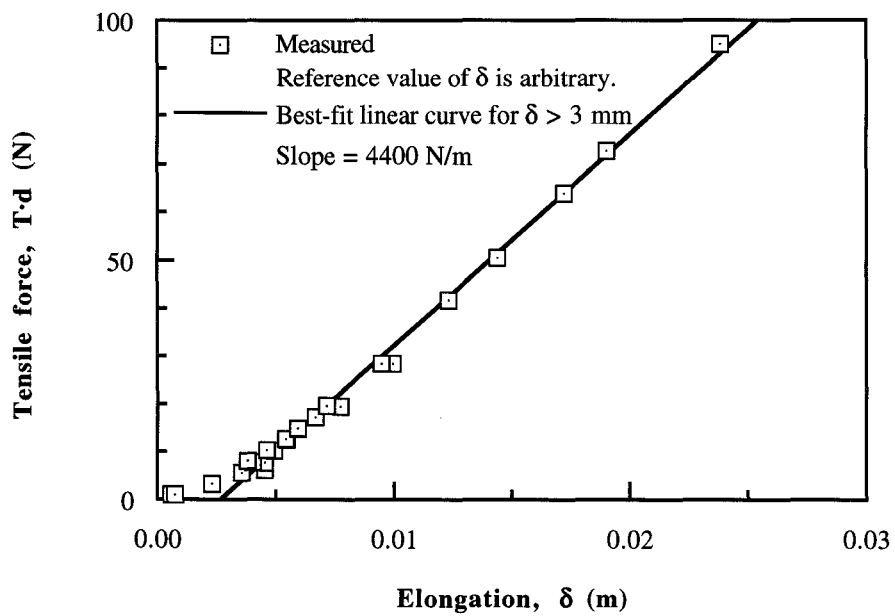Figure 6. Effects of web tension and supply pressure on out-of-plane stiffness (e = 0 mm)

Figure 7. Effects of web tension and supply pressure on longitudinal stiffness (e = 0 mm)

Figure 8. Effects of web tension and the gap between the upper and lower rows of air bars on longitudinal stiffness (p_o = 1240 Pa)

Figure 9. Tensile force and web elongation (d = 0.254 m, p_o = 0 Pa)
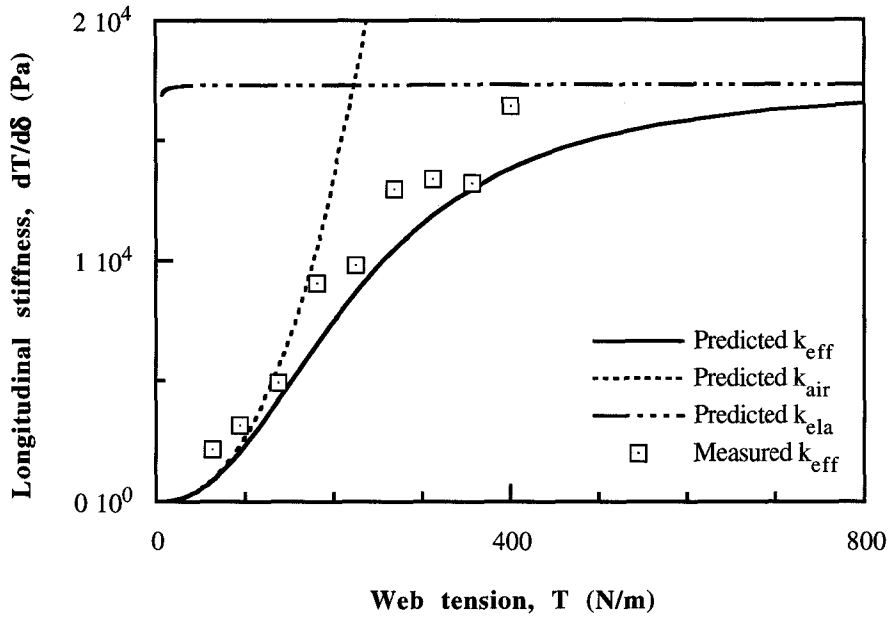
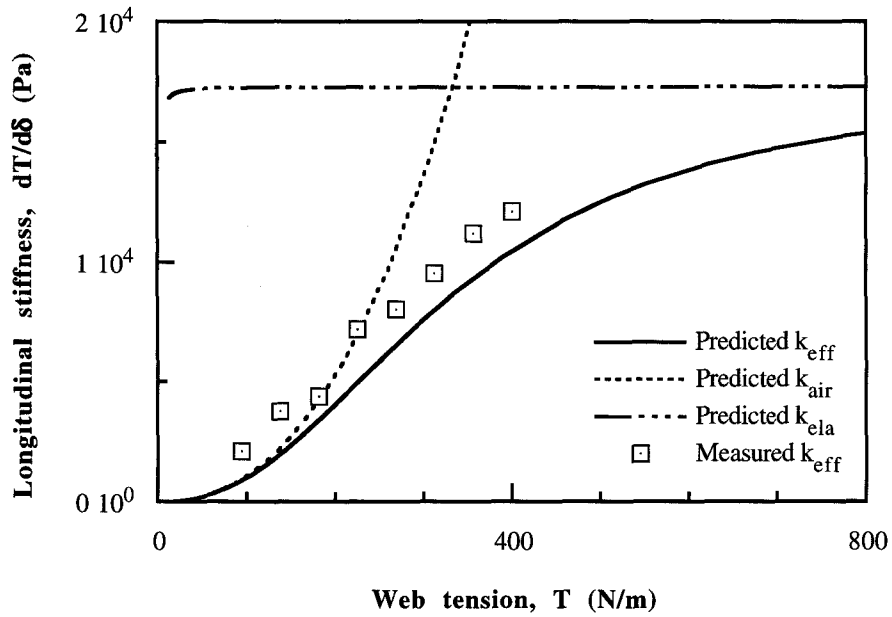Figure 10. Effect of web tension on longitudinal stiffness (e = 0 mm, p_o = 620 Pa)

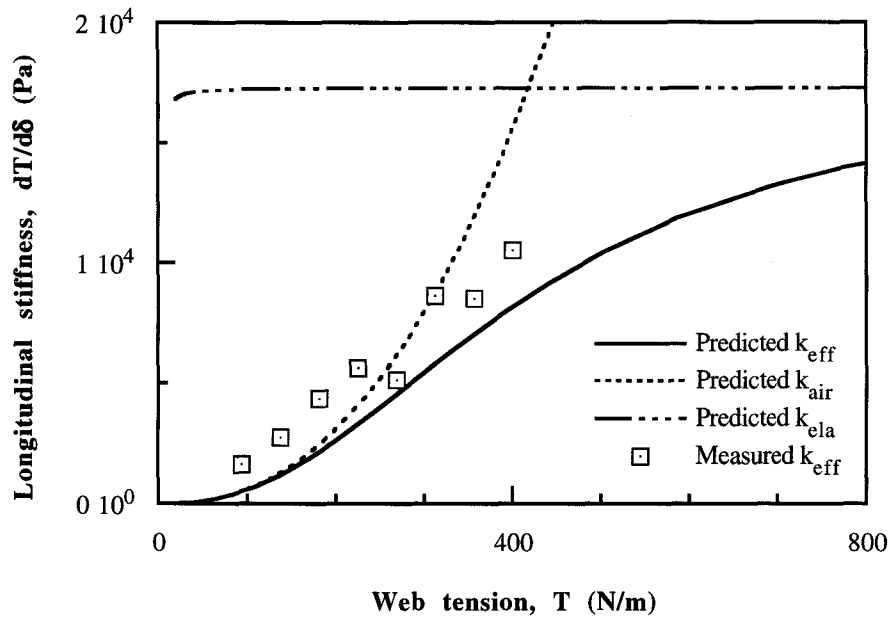Figure 11. Effect of web tension on longitudinal stiffness (e = 0 mm, p_o = 1240 Pa)

Figure 12. Effect of web tension on longitudinal stiffness (e = 0 mm, p_o = 1870 Pa)
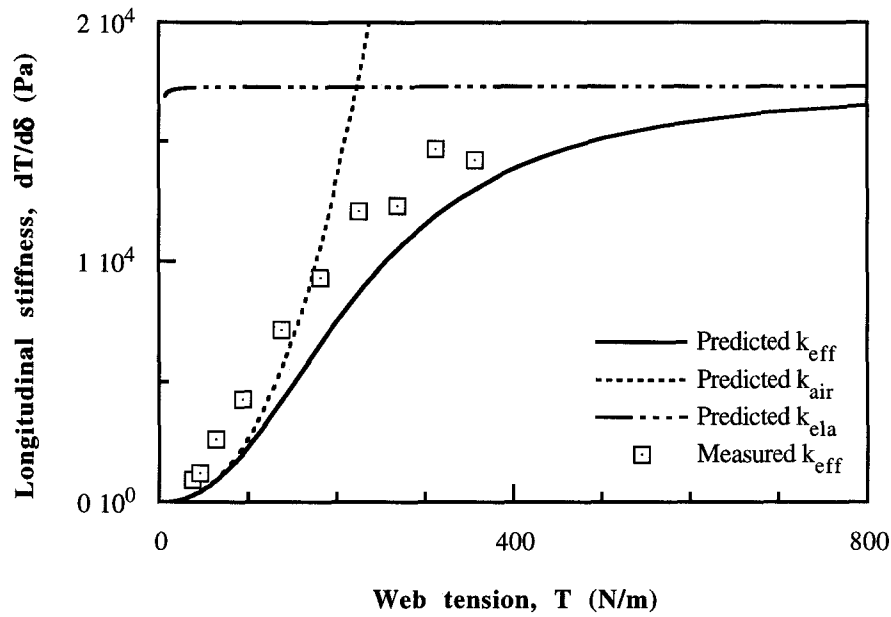

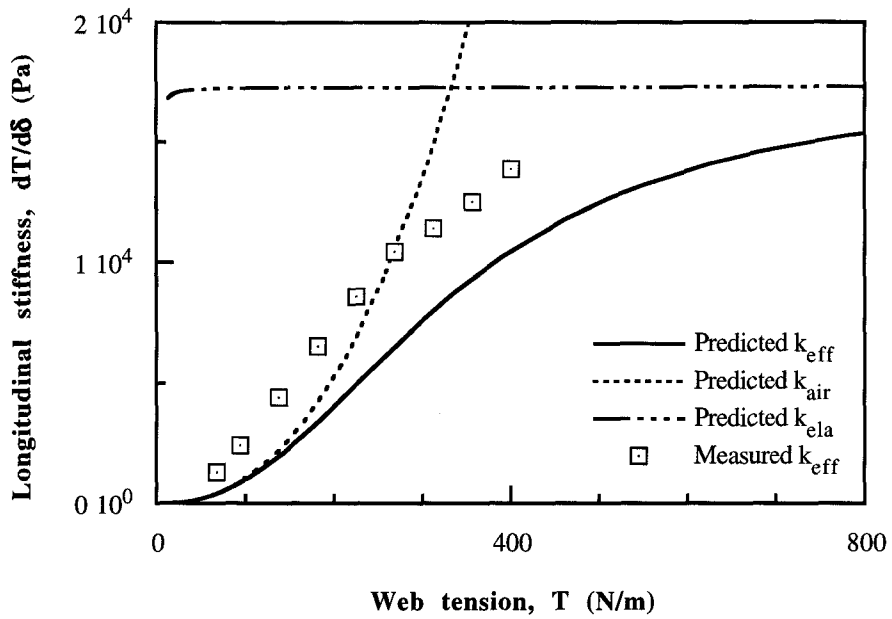Figure 13. Effect of web tension on longitudinal stiffness (e = 6.35 mm, p_o = 620 Pa)

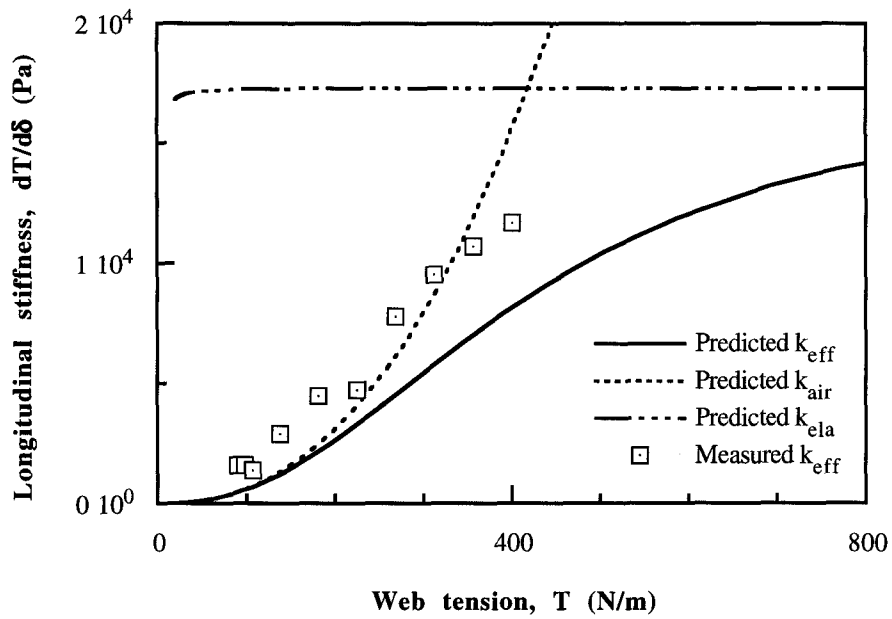Figure 14. Effect of web tension on longitudinal stiffness (e = 6.35 mm, p_o = 1240 Pa)

Figure 15. Effect of web tension on longitudinal stiffness (e = 6.35 mm, p_o = 1870 Pa)

Y. B. Chang, R. P. Swanson And P. M. Moretti
Resiliency of An Air-Floated Web
6/9/99   Session 4   1:00 - 1:25 p.m.

Question – Claude Faulkner, DuPont
Would you expect the stiffness to change much, if you considered a moving web and the possible accumulation of air associated with the web moving?

Answer – Y. B. Chang, Oklahoma State University
I think that depends on several things. If the supply pressure is not very high so that the air-jet velocities are low, and the web moves extremely fast, there could be an effect.

Question – Al Forrest, DuPont
I noticed in your setup to measure the stiffness, you had sort of a spring/mass system, and I was thinking that at some point you were going to displace the mass and let it vibrate to determine the natural frequency and compare it with what you would expect from the stiffness and the mass. Did you look into that?

Answer – Y. B. Chang, Oklahoma State University
Dr. Moretti may have something to say about that because during these experiments he was looking at the mass.

Comment – Peter Moretti, Oklahoma State University
We were testing the web as a spring by having a weight hanging from the end, I expected that when I put more weight on it, the frequency would keep going down. Well, I put on ten pounds, and twenty pounds, and the frequency stayed about the same; which told me this is a non-linear spring. So it was obvious even before we reduced the data, that we would get this hardening spring curve. However, we used the extension measurement to determine the force-versus-extension plot, rather than the natural frequency to find its slope.